Journal of Applied Electrochemistry (2006) 36:1253–1260
DOI 10.1007/s10800-006-9186-z

A DEMS study of the electrocatalytic hydrogenation and oxidation of *p*-dihydroxybenzene at polycrystalline and monocrystalline platinum electrodes

J. SANABRIA-CHINCHILLA[1], M.P. SORIAGA[1,*], R. BUSSAR[2] and H. BALTRUSCHAT[2]
[1]*Department of Chemistry, Texas A&M University, College Station, TX, 77843, USA*
[2]*Institut für Physikalische und Theoretische Chemie, Universität Bonn, D-53117, Bonn, Germany*
*(*author for correspondence, e-mail: soriaga@mail.chem.tamu.edu)*

Received 29 September 2005; accepted in revised form 3 May 2006

Key words: anodic oxidation of hydroquinone, chemisorption of hydroquinone, differential electrochemical mass spectrometry, electrochemical hydrogenation of hydroquinone

Abstract

The electrochemical hydrogenation and oxidation of *p*-dihydroxybenzene (hydroquinone) chemisorbed at polycrystalline Pt, well-ordered Pt(111) and disordered Pt(111) electrodes were studied by differential electrochemical mass spectrometry (DEMS). For comparative purposes, benzene was investigated at polycrystalline Pt. Anodic oxidation yielded only CO_2 as the volatile (DEMS-detectable) product. However, at least three oxidation cycles were necessary for exhaustive oxidation; this indicates that: (i) non-volatile products were generated in the first cycle, (ii) these products either stayed adsorbed or, in part, were re-adsorbed during a cathodic scan into the double-layer potential region, and (iii) these species were further oxidized on subsequent anodic scans. Electrocatalytic hydrogenation of hydroquinone at polycrystalline Pt followed two parallel (not sequential) paths to generate benzene and cyclohexane: the ''branching ratio'' was heavily in favor of the latter product. The adsorbate can be displaced by CO at potentials in the double layer region. Since no volatile species was observed during this process, the adsorbate is not already reduced; e.g., to benzene. On well-ordered Pt(111), no cyclohexane was produced and only a minuscule fraction of benzene was observed; however, quantitative desorption of (unidentified) non-volatile organic material took place at the negative potential. The disordered Pt(111) surface behaved more like the polycrystalline rather than the monocrystalline surface. The H_2Q-hydrogenation reaction proceeds more readily on Pt with surface steps and kinks.

1. Introduction

Studies on the chemisorption of organic compounds at catalytic surfaces have been aided by a proliferation of surface analytical methods [1–3] that can be applied to electrochemical systems. The extension of such studies to electrocatalytic reactions such as hydrogenation or oxidation is less straightforward because of the paucity of techniques that are able to provide qualitative and quantitative analysis of the (low-level) product distributions. The difficulty arises primarily from the fact that organic compounds do not undergo electrocatalytic reactions unless they are chemisorbed at the electrode surface. Unless ultrahigh-area surfaces such as porous or finely divided powder electrodes are used, the amounts of products generated are not only minuscule (ca. pmol cm^{-2}), they are also swamped by a huge excess of supporting electrolyte. The drawback in the employment of such surfaces is that they are ill-defined; hence, it is virtually impossible to obtain fundamental mechanistic information such as correlations between catalytic reactivities, surface sites and modes of chemisorption.

Studies on the orientation of chemisorbed molecules and its influence in electrochemical oxidation or reduction reactions were first attempted by indirect measurements using thin-layer electrochemistry (TLE) by Hubbard and coworkers [4, 5]. Central to the molecular orientation studies was the measurement of the surface coverage or packing density (Γ, mol/cm^2) of the intact chemisorbed molecules [6, 7]. Dihydroxy substituted benzene compounds were popular subject molecules because of the well-characterized electrochemistry [8–17]. The chemisorption isotherm of H_2Q on Pt(pc) surfaces has demonstrated that H_2Q chemisorption is a nonrandom, irreversible process in which chemisorbed species adopts specific orientations depending of the bulk organic solution. When chemisorption proceeds from diluted H_2Q solutions ($C < 0.10$ mM) flat-oriented species (η^6) is formed; whereas for solution with

concentrations higher than 1.0 mM, edgewise-oriented species (η^2) are formed. These orientational assignments have been verified using independent techniques such as infrared reflection-adsorption spectroscopy (IRAS) [18] and radiochemistry [19]. Studies on H_2Q chemisorption at well-defined Pt(111) surfaces have been reported as well [20, 21].

The effects of adsorbed-molecule orientation on the electrochemical oxidation and reduction of aromatic compounds were first studied on Pt electrodes [22–26]. The initial work involved a direct measurement of the number of electrons transferred during the oxidation (n_{ox}) or reduction (n_H) of adsorbed material by TLE. Gas chromatography (GC) with derivatization by silylation was employed to confirm oxidation products such as maleic acid [20]. Long optical path length thin-layer spectroelectrochemistry was employed to identify 1,4-cyclohexandiol as the product of the electrochemical reduction of H_2Q [27]. The use of the long optical path length and the large ratio of electrode area-to-solution volume were meaningful aspects in the detection of these species.

The development of differential electrochemical mass spectrometry (DEMS) has provided a major boost in the research area of electrochemical surface science. DEMS allows the identification and quantification of reaction product distributions. Equally critical is the fact that the product analysis can be directly linked to prominent features in a current–potential measurement: it is possible to record the electrochemical currents simultaneously with the mass spectrometer ion currents [28, 29]. DEMS has been successfully applied in the study of electrocatalytic hydrogenation of aromatic molecules. Examples are benzene on polycrystalline Pt [30], Pt(111) [31], Pt(110) and Pt(100) [32], and Pt(332) [33]; aniline and pyridine on polycrystalline and single-crystal Pt, Ru and Pd electrodes [34]; biphenyl, naphthalene and *t*-butylbenzene on Pt electrodes [35, 36]; benzyl alcohol [37]; and benzoic acid [38, 39] on Pd and Pt electrodes.

The present paper describes the application of DEMS on the electrocatalytic hydrogenation and oxidation of H_2Q at polycrystalline Pt(pc), well-ordered Pt(111) and disordered Pt(111). The former consists predominantly of surface terrace sites, whereas the disordered Pt(111) electrode would have an appreciable amount of surface defects (steps and kinks [1, 40–43]).

2. Experimental

The fabrication and utilization of a DEMS instrument has been described in detail elsewhere [28, 29]. In this study, a differentially pumped Balzers QMG 422 quadrupole mass spectrometer was employed; this set-up allows the simultaneous detection of up to 64 ion fragments. Electrochemistry was done in a one-compartment thin-layer cell.

Disk-shaped (polycrystalline and single-crystal) platinum electrodes were initially treated by immersion in 10 M HNO_3 (Merck) for at least 10 min. The Pt(pc) electrode was briefly flame-annealed to render it uniformly smooth. The Pt(111) single crystal was annealed for 3 min and quenched in an H-cell that contained 0.1 M H_2SO_4 under a stream of ultrapure argon (Air Products). The Pt(111) surface was disordered by multiple potential cycles between the hydrogen and oxygen evolution regions until a steady-state current–potential curve, devoid of the "butterfly peaks" characteristic of the well-ordered surface, was obtained. The electrodes were emersed and, with a protective drop of Ar-saturated supporting electrolyte, transferred into the DEMS thin-layer cell. The integrity of the electrode surfaces was always monitored prior to the adsorption experiments. The active surface areas of the working electrodes were determined from the hydrogen-adsorption (or desorption) Faradaic charges [2, 3, 5, 20]. A standard hydrogen electrode (SHE) in 0.1 M H_2SO_4 was used as the reference electrode.

Milli-Q® Plus water (Millipore Systems) was utilized to prepare all solutions which were deaerated with ultrapure argon. Hydroquinone (Merck) and benzene (Riedel-de Haën) solutions were prepared in 0.1 M H_2SO_4 at millimolar concentrations. Adsorption was performed by introduction of fresh adsorbate solution into the DEMS cell, at potentials in the double-layer region (0.35 V), followed by a 3-min equilibration. The cell was then rinsed copiously with pure supporting electrolyte to remove the unadsorbed material. The potential was scanned either in the anodic or cathodic direction without electrolyte flow. Multiple potential cycles were obtained until no more changes were observed in both the cyclic voltammograms (CV) and the mass spectra.

Calibration of the DEMS system was achieved as described elsewhere [28, 29]. Surface coverage data were estimated from integrated ion currents. (Note that the calibration constant, relating the ion current to the number of molecules entering the vacuum system, contains both the ionization probability and the fragmentation ratio of the corresponding ion.)

3. Results and discussion

Figure 1 shows simultaneous electrochemical CV and mass spectrometric cyclic voltammograms (MSCV) for H_2Q chemisorbed on Pt(pc) in a potential regime well above the hydrogen-evolution region. A potential-dependent intensity was found only for mass $m/z = 44$, which corresponds to CO_2. Although the second-cycle anodic-oxidation currents are only slightly larger than the background (Pt-surface-oxide-formation) currents, an appreciable amount of CO_2 was still detected by DEMS up to the third anodic scan. This result can only mean that: (a) there actually are non-volatile oxidation products that are retained in the DEMS thin-layer cell, (b) these non-CO_2 products are chemisorbed on the surface after the oxidized Pt is

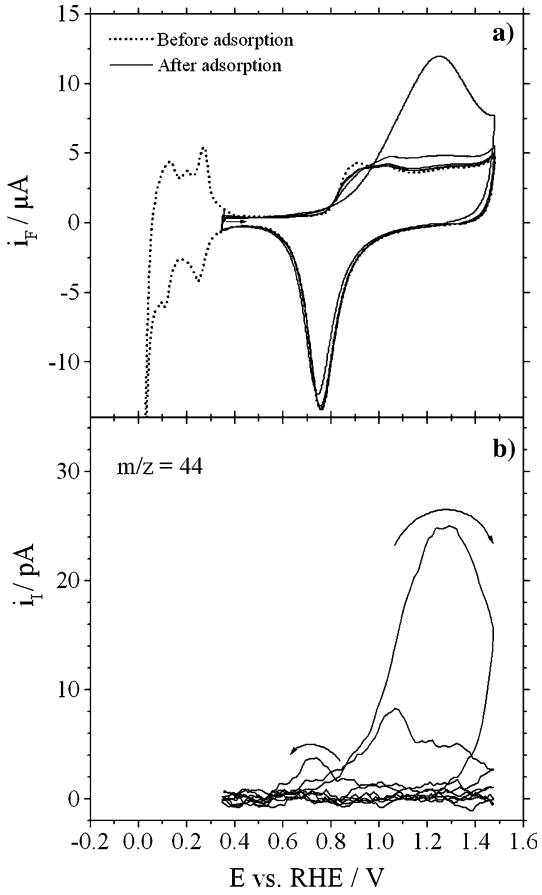

Fig. 1. (a) CV curve and (b) MSCV curve (m/z = 44, CO_2) for the anodic oxidation of a H_2Q-coated Pt(pc) electrode in H_2Q-free 0.1 M H_2SO_4. H_2Q was chemisorbed at 0.35 V. Scan rate = 10 mV s^{-1}.

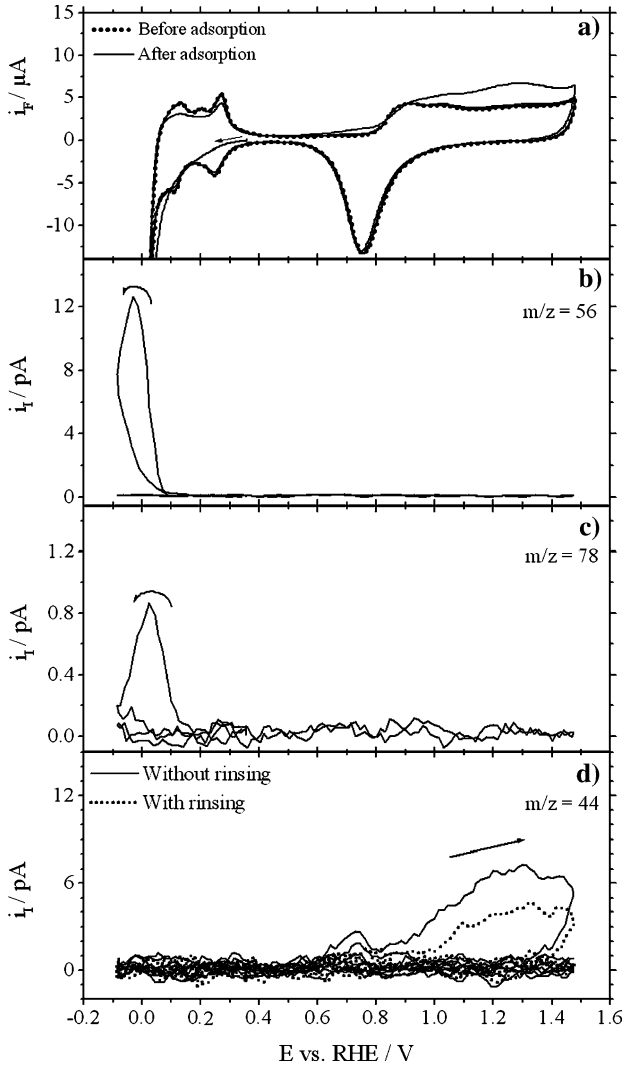

Fig. 2. (a) CV curve, (b) MSCV curve (m/z = 56, cyclohexane), (c) MSCV curve (m/z = 78, benzene), and (d) MSCV curve (m/z = 44, CO_2) for the electrochemical hydrogenation of a H_2Q-coated Pt(pc) electrode in H_2Q-free 0.1 M H_2SO_4. All other experimental conditions were as in Figure 1.

reverted to its metallic form, and (c) the adsorbed products are eventually oxidized exhaustively (to CO_2) on subsequent anodic cycles, consuming a lower number of electrons per CO_2 formed than in the first sweep which results in a smaller faradaic-to-ion-current ratio. A similar behavior had been observed previously for other aromatic systems such as toluene, benzene and biphenyl [31, 33, 44].

The cycle-dependent percent yields of CO_2 were determined from the areas under the CO_2 mass peaks in Figure 1. (The currents beyond the third sweep are identical to those obtained from the pure supporting electrolyte; hence, they were used for the background correction.)

Eighty percent of the total CO_2 yield was generated in the first anodic scan, 17% in the second sweep, and 3% in the third cycle. No information is available that would permit the identification of the non-volatile species that remained in the DEMS thin-layer cell after the first cycle. The possibility exists that 20% of the organic may have been partially oxidized to a shorter-chain unsaturated species; for example, maleic acid was detected in the anodic oxidation of hydroquinone on polycrystalline Pt [5, 20]. On the other hand, for benzene and toluene, a similar behavior has been observed in the "classical" DEMS cell [44] where a porous electrode is used at the bottom of a cylindrical cell with a height of several centimeters; dissolved products are therefore free to diffuse away into the bulk of the electrolyte. It has been concluded that some carbonaceous species stay absorbed (and, possibly, are buried below the PtO during the place exchange between Pt and O) [44]. This may also be true for H_2Q.

Figure 2 shows CV and MSCV data for the hydrogenation of H_2Q; here, the potential sweep was initiated in the negative direction. Only two hydrogenation products, cyclohexane (m/z = 56) and benzene (m/z = 78), were detected by DEMS. It is important to note that the two mass peaks occur at almost the same potential, a result that suggests that the hydrogenation of H_2Q to cyclohexane and benzene involves two *parallel* mechanistic paths. In other words, the reaction is *not sequential* as in $H_2Q_{(ads)} \rightarrow C_6H_{6(ads)} \rightarrow C_6H_{12(ads)}$. This does not exclude the possibility that, in the reaction path leading to cyclohexane, adsorbed

Table 1. Amounts of desorption products from H_2Q and benzene adsorbates on Pt(pc)

Detected species	Cathodic sweep				Anodic sweep	
	Γ/nmol cm^{-2}				Γ/nmol cm^{-2}	n_{ox}
Adsorbate/surface	Cyclohexane	Benzene	CO_2	Total C_6	(total, from CO_2)	
Hydroquinone/Pt(pc)	0.095	0.004	0.063 * 6	0.16	0.28	5.2
Hydroquinone/Pt(111)	0.00	0.002	0.175 * 6	0.18	0.19	5.3
Hydroquinone/rough Pt(111)	0.07	0.003	0.092 * 6	0.17	–	–
Benzene/Pt(pc)	0.11	0.043	0.064 * 6	0.22	0.30	5.2

benzene is formed as a short-lived intermediate which does not desorb. The hydrogenation "branching ratio" is heavily in favor of the saturated product as the cyclohexane:benzene ratio (taking into account the differing sensitivities) is approximately 26:1 (Figure 2b, c and Table 1). The likelihood of two parallel mechanisms is further supported by the fact that, in order for benzene to be hydrogenated, it must remain chemisorbed on the surface [5, 20, 21, 25].

It can be seen from Figure 2d that a small but noticeable CO_2 peak appears in the MSCV curve in the first post-hydrogenation anodic scan. This is an indication that there is a small fraction of organic that remains on the surface and/or in the solution during the hydrogenation reaction; these species are the ones that undergo anodic oxidation to CO_2 on the ensuing anodic scan. That both surface and unadsorbed materials exist is confirmed by an experiment that, if the DEMS thin-layer cell is rinsed with pure supporting electrolyte at -0.1 V (to remove any non-surface-attached species), a CO_2 mass peak is still observed, albeit at a smaller quantity (cf., dotted line in Figure 2d). Therefore, a small part of the adsorbate might desorb as a non-volatile species, possibly H_2Q itself or 1,4-cyclohexanediol; it has also been reported that hydrogenation of chemisorbed H_2Q at thermally smoothened Pt(pc) with a copious amount of $H_{2(g)}$ yields 1,4-cyclohexanediol [25]. That part of the adsorbate which is not desorbed at low potentials might be due to molecules bound strongly to sites of a particular surface orientation. For comparison, whereas benzene is completely desorbed from most surfaces at low potentials, either under hydrogenation or without, from Pt(100) less than half of the adsorbate can be desorbed [32].

For comparative purposes, the electrocatalytic hydrogenation of benzene chemisorbed on Pt(pc) was also investigated in the identical cell and under identical conditions. The results, in terms of CV and MSCV data, are shown in Figure 3. When scrutinized in relation to the observations in Figure 2, three major differences emerge: (i) The MSCV peak for cyclohexane has not only increased, but is also of a different morphology. (ii) The benzene mass peak has increased substantially; its onset is shifted to 0.3 V. The cyclohexane-to-benzene peak-area ratio obtained from the hydrogenation of H_2Q is approximately ten-fold larger than that measured from the hydrogenation of benzene. (iii) The time (or potential) lag for cyclohexane production relative to the benzene desorption is much more pronounced. In [33], it was described an experiment, where after adsorption of benzene on Pt(332) the potential was held at 70 mV for 5 min, only $m/z = 78$ was observed. After continuation of the sweep in the negative direction, mostly cyclohexane and only traces of benzene were

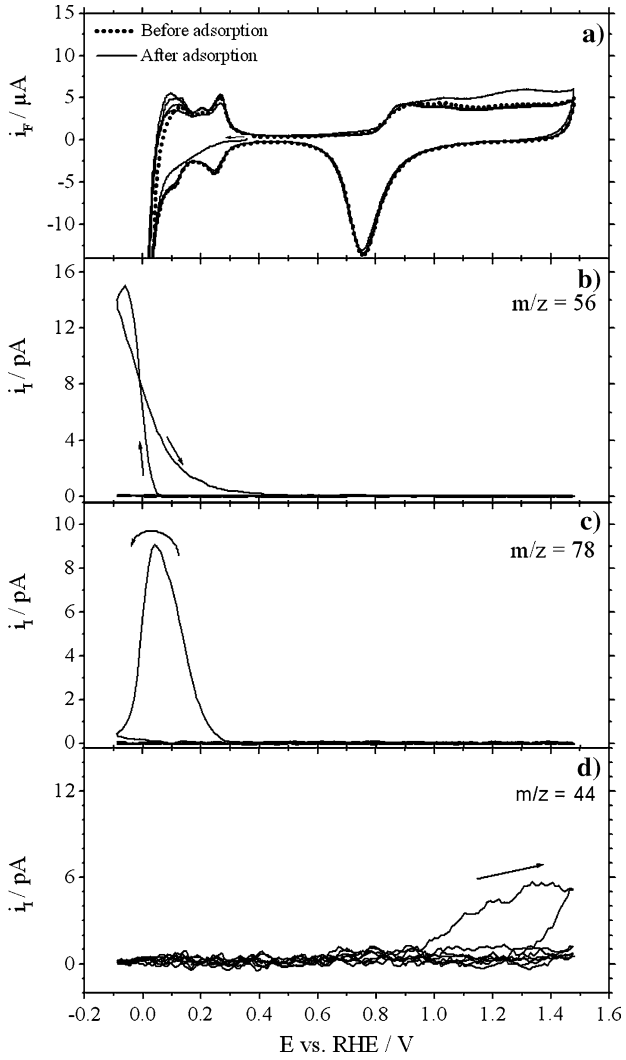

Fig. 3. (a) CV curve, (b) MSCV curve ($m/z = 56$, cyclohexane), (c) MSCV curve ($m/z = 78$, benzene), and (d) MSCV curve ($m/z = 44$, CO_2) for the electrochemical hydrogenation of a benzene-coated Pt(pc) electrode in benzene-free 0.1 M H_2SO_4. All other experimental conditions were as in Figure 1.

observed. The total amounts of benzene and cyclohexane were identical to those observed during a continuous sweep. Therefore, the original adsorption site determines which species is formed at low potentials. Since in the case of H_2Q, benzene and cyclohexane are formed at nearly identical potentials, this is further evidence that the H_2Q hydrogenation to cyclohexane and benzene transpires along two parallel, not sequential, pathways:

$$H_2Q_{(ads)} \xrightarrow[Pt(pc)]{\text{Hydrogenation}} \text{Cyclohexane}_{(aq)} + \text{Benzene}_{(aq)} + \text{Non-volatile products} \quad (2)$$

It may be noted in Figure 3d that a small but measurable CO_2 mass peak appears in a subsequent anodic scan; since possible hydrogenated products of benzene are volatile, incomplete desorption is thus indicated for benzene.

A comparison of the amounts of desorbing species, calculated from the integrated ion currents, is given in Table 1. Values obtained from cathodic desorption experiments are lower than those obtained from the amount of CO_2 when the first sweep was in the anodic direction. For benzene, it has been observed that several sweeps, restricted to the hydrogen region, are necessary for a complete hydrogenation of the adsorbate; up to 30% of the total cyclohexane are desorbed only in those subsequent sweeps [30]. In the case of H_2Q, this relative amount may even be larger. Even without an electrolyte exchange at the negative potential limit, some of the species may be lost due to a constant, small flow of electrolyte and diffusion into the capillaries of the cell, and thus not oxidized to CO_2.

A priori, one cannot exclude that H_2Q is already reduced to adsorbed benzene upon adsorption, in particular on polycrystalline Pt. From the different morphology of the ion current transient for cyclohexane formed after adsorption of H_2Q and benzene, one may already exclude this possibility. To further prove that this is not the case, displacement experiments were carried out using CO. After H_2Q adsorption at 0.35 V, a CO-saturated 0.1 M H_2SO_4 solution was passed through the cell under potential control (0.25 V) using a flow rate of 0.70 μl s^{-1}. Such a slow flow rate was used to guarantee that the desorbed species have enough time to diffuse from the electrode surface to the membrane and

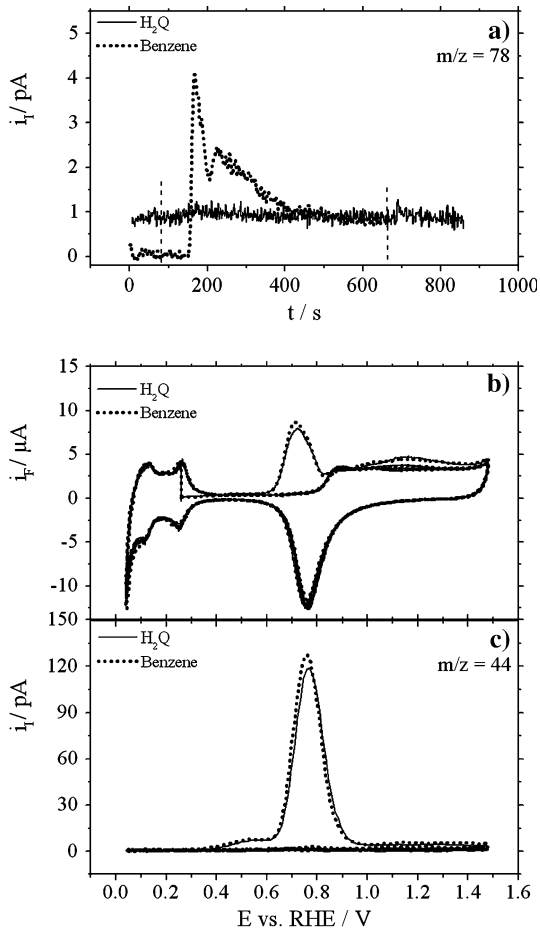

Fig. 4. (a) Ion current transients of m/z = 78 during the displacement of H_2Q- and benzene-coated Pt(pc) electrodes by CO adsorption, (m/z = 78, benzene). (b) CV after CO adsorption, same conditions as in Figure 1. (c) MSCV (m/z = 44, CO_2).

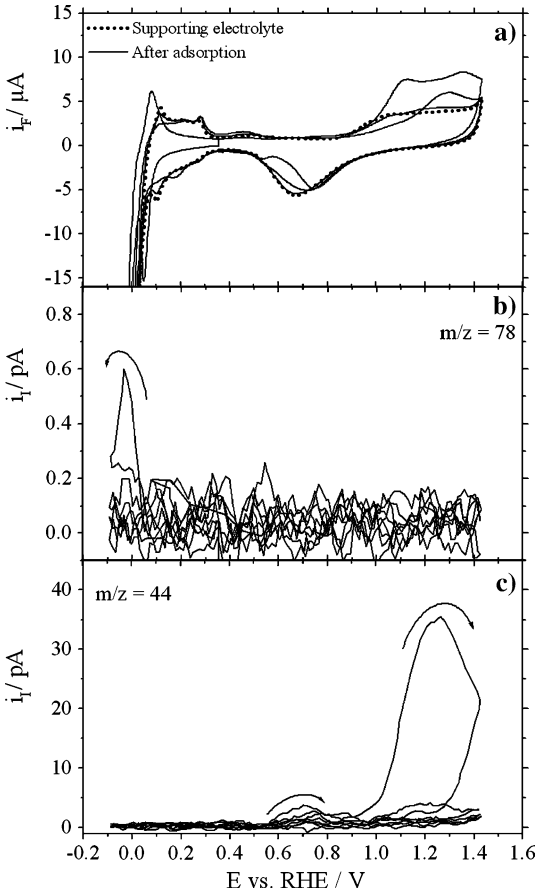

Fig. 5. (a) CV curve, (b) MSCV (m/z = 78, benzene), and (c) MSCV curve (m/z = 44, CO_2) for the electrochemical hydrogenation of a H_2Q-coated Pt(111) electrode in H_2Q-free 0.1 M H_2SO_4. All other experimental conditions were as in Figure 1.

reach the mass spectrometer instead of leaving the cell with the solution. As was expected, no active signals were detected during the displacement since it is not possible to detect H_2Q using DEMS.

Control experiments were performed displacing pre-adsorbed benzene at the same H_2Q experimental conditions. Figure 4 summarizes the results of the H_2Q and benzene displacement experiments. The ion–current transient in Figure 4a shows benzene (m/z = 78) during the introduction of the CO-saturated solution into the thin-layer DEMS cell. Figure 4b, c show the CV and MSCV recorded after the displacement experiments and electrolyte exchange. The CV shows the suppression of the hydrogen region at 0.25 V due to CO adsorption. The voltammetric feature at 0.70 V corresponds to the CO oxidation as can be extracted from the MSCV. In addition, a small contribution of aromatic-like species was observed in the region between 1.00 V and 1.40 V indicating the oxidation of the remaining aromatic adsorbate. The amount of displaced adsorbate by CO was estimated to be 90% for H_2Q; in comparison, 97% of the original benzene adlayer was displaced in the second experiment. The surface coverage of benzene was calculated to be 0.26 nmol cm^{-2}.

Figure 5 shows CV and MSCV results for the H_2Q hydrogenation, initiated by a cathodic scan, and subsequent anodic oxidation of the chemisorbed adlayer on a well-ordered Pt(111) surface. The two most significant observations are: (i) No cyclohexane was produced; only benzene, in minuscule quantities, was detected by DEMS. (ii) A large amount of CO_2, essentially as much as that for H_2Q on Pt(pc) without prior hydrogenation (cf. Figure 1d), was generated. These results both point to the relative inactivity of the well-ordered Pt(111) surface towards electrocatalytic hydrogenation of H_2Q to cyclohexane and/or benzene. Presumably, because the polycrystalline surface contains an appreciable amount of steps and/or kinks [1], it is much more aggressive towards H_2Q hydrogenation than a well-ordered hexagonally close-packed surface.

The fact that, in the experiment of Figure 5b, cyclohexane is not produced, or that benzene is generated only to an almost negligible extent, does not necessarily mean that the well-ordered Pt(111) surface is totally

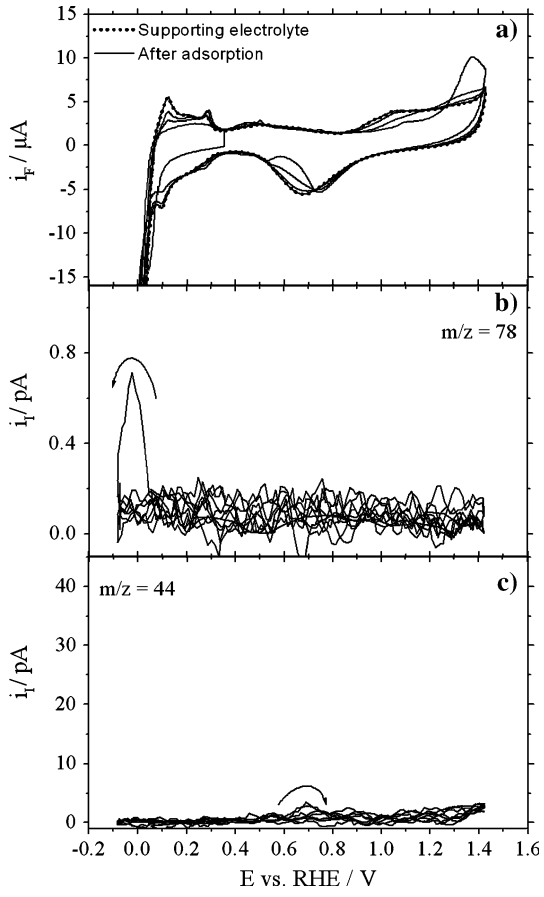

Fig. 6. (a) CV curve, (b) MSCV (m/z = 78, benzene), and (c) MSCV curve (m/z = 44, CO_2) for the electrochemical hydrogenation of a H_2Q-coated Pt(111) electrode in H_2Q-free 0.1 M H_2SO_4. The DEMS thin-layer cell was rinsed at −0.10 V prior to the anodic scan. All other experimental conditions were as in Figure 1.

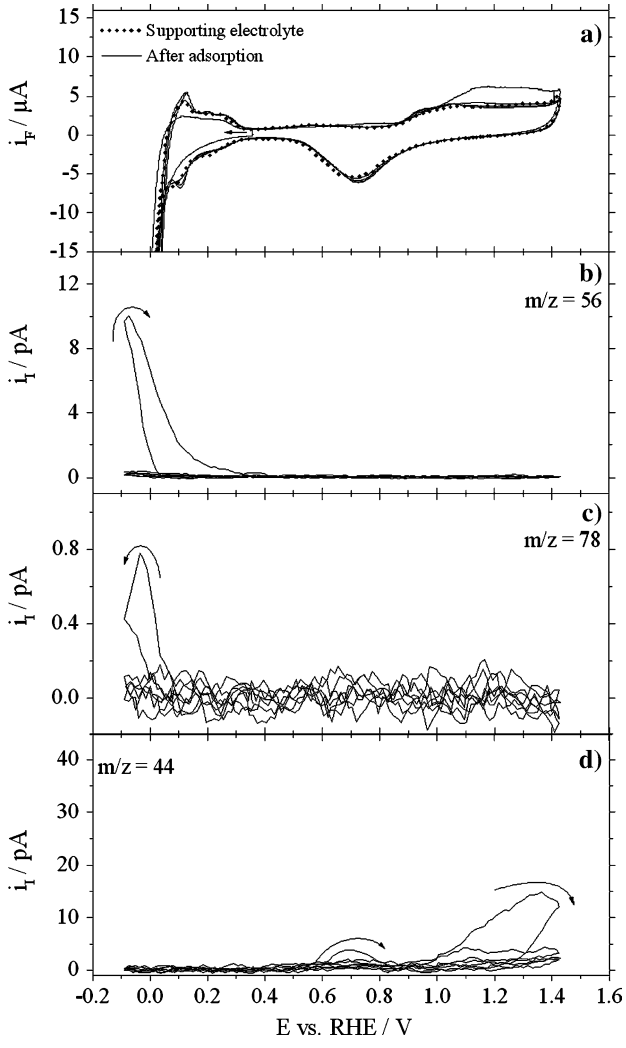

Fig. 7. (a) CV curve, (b) MSCV (m/z = 78, benzene), and (c) MSCV curve (m/z = 44, CO_2) for the electrochemical hydrogenation of H_2Q-coated disordered Pt(111) electrode in H_2Q-free 0.1 M H_2SO_4. All other experimental conditions were as in Figure 1.

devoid of interfacial reactions, whether it is hydrogenation or simple electro-desorption. This may be inferred from the data in Figure 6, where the DEMS thin-layer cell was rinsed with pure supporting electrolyte at -0.1 V. Since no CO_2 mass peak appears on the subsequent anodic scan, it is clear that non-volatile material was quantitatively desorbed from the surface, and rinsed away, at the negative potential. Furthermore, the cathodic peak around 0.05 V in Figures 5 and 6 indicates displacement of the original H_2Q adsorbate by adsorbed hydrogen. It must be noted that, contrary to the experiments at Pt(pc), no CO_2 was formed in the subsequent anodic sweep; desorption therefore was complete.

In comparison, oxidation of benzene adsorbed at Pt(111) proceeds in two steps, only the second of which is paralleled by CO_2 formation [31]. From the oxidation-charge values, it is suggested that adsorbed hydroquinone/quinone species are formed in the first step, which, upon reversal of the sweep in the cathodic direction, are desorbed in a sharp peak prior to hydrogen evolution. The similar desorption behavior and peak shape in the present study corroborate this interpretation.

The above experiments were repeated with a Pt(111) surface that had been disordered by multiple electrochemical oxidation and reduction cycles; the aim was to introduce (mild) surface disorder and ascertain its effect on H_2Q hydrogenation. The CV and MSCV results are given in Figure 7. It is not difficult to note that the features in this figure are quite similar to those at Pt(pc) (cf. Figure 2), but profoundly different from those at well-ordered Pt(111); specifically, both cyclohexane and benzene are generated on the disordered surface but not on the well-ordered single-crystal electrode. Evidently, a slightly roughened Pt(111) behaves more like a polycrystalline rather than a monocrystalline platinum surface, at least in terms of H_2Q hydrogenation. It also appears that the latter reaction proceeds more readily at Pt surfaces that contain surface defects such as steps and kinks. A similar effect was earlier observed for the hydrogenative desorption of ethene from a roughened Pt(111) [42] and of benzene from a stepped Pt(332) [33]. The different shape of the cyclohexane signal (majority of the species is detected only in the subsequent anodic scan) may indicate a slower desorption of cyclohexane than on Pt(pc). However, the desorption starts at potentials where hydrogen evolution is strong; since the resulting iR-drop in the thin layer cell is considerable, the actual potential at the negative potential limit (on which the desorption rate strongly depends) is not well defined.

The amount of species detected upon desorption from Pt(111) is also included in Table 1. It is smaller than that observed for Pt(pc) or roughened Pt(111), in accordance with the previous observations [21]. The corresponding coverage is lower than that obtained from Auger electron spectroscopy (0.3 nmol cm^{-2} [21]) and much lower than that calculated from the structure observed by STM (0.38 nmol cm^{-2}, [45]). Although this difference may partly be caused by losses due to desorption and experimental errors, changes in pH, differences in supporting electrolyte and, in particular, the presence of H_2Q may also lead to variable surface coverages. Moreover, it must be noted that coverages extracted from structure determinations are ideal values which, on real surfaces, are lowered due to domain boundaries and other imperfections.

4. Conclusions

The electrocatalytic hydrogenation and oxidation of hydroquinone chemisorbed on polycrystalline Pt, well-ordered Pt(111), and disordered Pt(111) surfaces were studied by DEMS. For comparative purposes, benzene was investigated at polycrystalline Pt. Anodic oxidation yielded only CO_2 as the volatile (DEMS-detectable) product. However, at least three oxidation cycles were necessary for exhaustive oxidation; this indicates that: (i) non-volatile products were generated in the first cycle, (ii) these products were re-adsorbed during a cathodic scan into the double-layer potential region, and (iii) the re-chemisorbed species were further oxidized on subsequent anodic scans. Electrocatalytic hydrogenation of H_2Q at Pt(pc) followed two parallel (not sequential) paths to generate benzene and cyclohexane: the ''branching ratio'' was heavily in favor of the latter product. On well-ordered Pt(111), no cyclohexane was produced and only a minuscule fraction of benzene was observed; however, quantitative desorption of (unidentified) non-volatile organic material took place at the negative potential. The disordered Pt(111) surface behaved more like the polycrystalline rather than the monocrystalline surface. The H_2Q-hydrogenation reaction proceeds more readily on Pt with surface steps and kinks.

It is interesting to note that, whereas H_2Q is irreversibly reduced to benzene and cyclohexane on polycrystalline Pt, there is strong indication that, on Pt(111), benzene can be (irreversibly) oxidized to adsorbed H_2Q [31].

Acknowledgements

The present project was funded by the Deustche Forschungsgemeinschaft (DFG). MPS would like to acknowledge the Welch Foundation for additional support. JSC thanks the German Academic Exchange Service (DAAD) for a research fellowship to conduct DEMS experiments in the laboratories of HB.

References

1. G.A. Somorjai, *Introduction to Surface Chemistry and Catalysis* (Wiley, New York, 1994).
2. M.P. Soriaga, D.A. Harrington, J.L. Stickney and A. Wieckowski. *in* B.E. Conway, R.E. White and J.O'M. Bockris (eds), Modern Aspects of Electrochemistry, (Plenum, New York, 1966).

3. A.J. Bard, H.D. Abruña, C.E. Chidsey, L.R. Faulkner, S. Feldberg, K. Itaya, O. Melroy, R.W. Murray, M.D. Porter, M.P. Soriaga and H.S. White, *J. Phys. Chem.* **97** (1993) 7147.
4. M.P. Soriaga and A.T. Hubbard, *J. Am. Chem. Soc.* **104** (1982) 2735.
5. M.P. Soriaga, E. Binamira-Soriaga, A.T. Hubbard, J.B. Bezinger and K.-W.P. Pang, *Inorg. Chem.* **24** (1985) 65.
6. A.T. Hubbard, *Chem. Rev.* **88** (1988) 633.
7. M.P. Soriaga, *Chem. Rev.* **90** (1990) 771.
8. M.P. Soriaga, P.H. Wilson and A.T. Hubbard, *J. Electroanal. Chem.* **142** (1982) 317.
9. M.P. Soriaga and A.T. Hubbard, *J. Am. Chem. Soc.* **104** (1982) 3937.
10. M.P. Soriaga, J.H. White and A.T. Hubbard, *J. Phys. Chem.* **87** (1983) 3048.
11. M.P. Soriaga and A.T. Hubbard, *J. Phys. Chem.* **88** (1984) 1089.
12. M.P. Soriaga, V.K.F. Chia, J.H. White, D. Song and A.T. Hubbard, *J. Electroanal. Chem.* **162** (1984) 143.
13. V.K.F. Chia, M.P. Soriaga and A.T. Hubbard, *J. Electroanal. Chem.* **167** (1984) 97.
14. M.P. Soriaga, J.H. White, D. Song and A.T. Hubbard, *J. Electroanal. Chem.* **171** (1984) 359.
15. J.H. White, M.P. Soriaga and A.T. Hubbard, *J. Electroanal. Chem.* **177** (1984) 89.
16. M.P. Soriaga, D. Song and A.T. Hubbard, *J. Phys. Chem.* **89** (1985) 285.
17. M.P. Soriaga, D. Song, D.C. Zapien and A.T. Hubbard, *Langmuir* **1** (1985) 123.
18. K.P. Pang, J.B. Benziger, M.P. Soriaga and A.T. Hubbard, *J. Phys. Chem.* **88** (1984) 4583.
19. E.K. Krauskopf and A. Wieckowski, *J. Electroanal. Chem.* **296** (1990) 159.
20. M.P. Soriaga, J.H. White, D. Song, V.K. Chia, P.O. Arrhenius and A.T. Hubbard, *Inorg. Chem.* **24** (1985) 73.
21. J.Y. Gui, B.E. Kahn, L. Laguren-Davidson, C.-H. Lin, F. Lu, G.N. Salaita, D.A. Stern and A.T. Hubbard, *Langmuir* **5** (1989) 819.
22. T. Mebrahtu, G.M. Berry and M.P. Soriaga, *J. Electroanal. Chem.* **247** (1988) 241.
23. M.P. Soriaga, J.L. Stickney and A.T. Hubbard, *J. Mol. Cat.* **21** (1983) 211.
24. M.P. Soriaga, J.L. Stickney and A.T. Hubbard, *J. Electroanal. Chem.* **144** (1983) 207.
25. T. Mebrahtu, G.M. Berry and M.P. Soriaga, *J. Electroanal. Chem.* **239** (1988) 375.
26. B. Bravo, S.L. Michelhaugh, T. Mebrahtu and M.P. Soriaga, *Electrochim. Acta* **11** (1988) 1507.
27. Y-P. Gui and T. Kuwana, *Langmuir* **2** (1986) 471.
28. H. Baltruschat. *in* A. Wieckowski (Ed), Interfacial Electrochemistry, (Marcel Dekker, New York, 1999).
29. H. Baltruschat, *J. Am. Soc. Mass Spectrom.* **15** (2004) 1693.
30. T. Hartung and H. Baltruschat, *Langmuir* **6** (1990) 953.
31. T. Hartung, U. Schmiemann, I. Kamphausen and H. Baltruschat, *Anal. Chem.* **63** (1991) 44.
32. U. Schmiemann and H. Baltruschat, *J. Electroanal. Chem.* **347** (1993) 93.
33. T. Löffler, R. Bussar, E. Drbalkova, P. Janderka and H. Baltruschat, *Electrochim. Acta* **48** (2003) 3829.
34. U. Schmiemann, Z. Jusys and H. Baltruschat, *Electrochim. Acta* **39** (1994) 561.
35. J. Vestral, Th. Lofflër, U. Müller and H. Baltruschat, *J. Electroanal. Chem.* **461** (1999) 90.
36. T. Löffler, E. Drbalkova, P. Janderka, P. Königshoven and H. Baltruschat, *J. Electroanal. Chem.* **550** (2003) 81.
37. J.L. Rodríguez, R.M. Souto, S. González and E. Pastor, *Electrochim. Acta* **44** (1998) 1415.
38. R.M. Souto, J.L. Rodríguez, L. Fernández-Mérida and E. Pastor, *J. Electroanal. Chem.* **494** (2000) 127.
39. R.M. Souto, J.L. Rodríguez, G. Pastor and E. Pastor, *Electrochim. Acta* **45** (2000) 1645.
40. F.T. Wagner and P.N. Ross, *J. Electroanal. Chem.* **150** (1983) 141.
41. J. Clavilier, A. Rodes, K.E. Achi and M.A. Zamakhchari, *J. Chim. Phys.* **88** (1991) 1291.
42. T. Löffler and H. Baltruschat, *J. Electroanal. Chem.* **554–555** (2003) 333.
43. K. Sashikata, N. Furuya and K. Itaya, *J. Vac. Sci. Technol. B* **9** (1991) 457.
44. J.M. Zhu, T. Hartung, D. Tegtmeyer, H. Baltruschat and J. Heitbaum, *J. Electroanal. Chem.* **244** (1988) 273.
45. J. Inukai, M. Wakisaka, M. Yamagishi and K. Itaya, *Langmuir* **20** (2004) 7507.